Clinical & Experimental Metastasis (2025) 42:25
https://doi.org/10.1007/s10585-025-10343-4

RESEARCH PAPER

A new, immunocompetent brain-metastatic mouse model of HER2-positive breast cancer

Leran Chen[1] · Angela Chow[1] · Wanchao Ma[1] · Courtney Coker[1] · Yifan Gu[1,5] · Peter Canoll[2,3] · Manoj Kandpal[4] · Hanina Hibshoosh[2,3] · Anup K. Biswas[1,2] · Swarnali Acharyya[1,2,3]

Received: 11 January 2025 / Accepted: 26 March 2025

Abstract

Brain metastasis is a common and devastating complication of cancer that affects over 50% of HER2-positive ($HER2^+$) breast cancer patients. The lack of effective long-term treatment options for brain metastasis significantly increases morbidity and mortality among these patients. Therefore, understanding the underlying mechanisms that drive brain metastasis is critically important for developing new strategies to treat it effectively. Genetically engineered mouse models (GEMMs) of $HER2^+$ breast cancer have been instrumental in understanding the development and progression of $HER2^+$ breast cancer. However, the GEMM models for $HER2^+$ breast cancer do not develop brain metastasis and are not suitable for the study of brain metastasis. We therefore developed a fully immunocompetent mouse model of experimental brain metastasis in $HER2^+$ breast cancer by injecting a murine HER2/neu-expressing mammary-tumor-cell line into the arterial circulation of syngeneic FVB/N mice followed by isolation of brain-metastatic derivatives through in-vivo selection. By this in-vivo serial passaging process, we selected highly brain-metastatic (BrM) derivatives known as neu-BrM. Notably, after intracardiac injection, neu-BrM cells generated brain metastasis in 100% of the mice, allowing us to study the later stages of metastatic progression, including cancer-cell extravasation and outgrowth in the brain. Analogous to human brain metastasis, we observed reactive gliosis and significant immune infiltration in the brain tissue of mice injected with neu-BrM cells. We further confirmed that brain-metastatic lesions in the neu-BrM model express HER2. Consistently, we found that the brain-metastatic burden in these mice can be significantly reduced but not eliminated with tucatinib, an FDA-approved, blood-brain-barrier-penetrant HER2 inhibitor. Therefore, the neu-BrM $HER2^+$ breast cancer model can be used to investigate the roles of innate and adaptive immune-system components during brain-metastatic progression and the mechanisms of HER2-therapy response and resistance.

Keywords Brain metastasis · HER2-positive breast cancer

Leran Chen and Angela Chow contributed equally to this work and first authors.

Wanchao Ma and Courtney Coker contributed equally to this work and second authors.

✉ Swarnali Acharyya
sa3141@cumc.columbia.edu

[1] Institute for Cancer Genetics, Columbia University Irving Medical Center, 1130 St Nicholas Avenue, New York, NY 10032, USA

[2] Department of Pathology and Cell Biology, Columbia University Irving Medical Center, 630 W 168th St, New York, NY 10032, USA

[3] Herbert Irving Comprehensive Cancer Center, Columbia University Irving Medical Center, 1130 St. Nicholas Ave, New York, NY 10032, USA

[4] Center for Clinical and Translational Science, Rockefeller University Hospital, 1230 York Ave, New York, NY 10065, USA

[5] Present address: 111 Biological Science Building, 484 W, 12th Avenue, Columbus, OH 43210, USA

Published online: 12 April 2025

Introduction

Brain metastasis represents a major clinical challenge that is associated with poor patient prognosis and limited therapeutic options. The incidence of brain metastasis in cancer patients is the highest in lung cancer, breast cancer and melanoma [1, 2]. Among breast-cancer subtypes, patients with triple-negative and $HER2^+$ breast cancers have the highest frequency of brain metastasis (30-50%) [3–5]. In the case of $HER2^+$ breast cancers, although new brain-penetrant HER2-targeted therapies have delayed brain-metastasis progression, clinical responses are often not durable and result in fatal relapses [6, 7]. Therefore, it is important to understand the underlying biological mechanisms that drive brain metastasis in $HER2^+$ breast cancer so that more effective and durable therapeutic solutions can emerge.

Genetically engineered mouse models (GEMMs) of $HER2^+$ breast cancer have provided invaluable insights into the process of breast tumorigenesis; yet, the usefulness of GEMMs for studying breast cancer metastasis is limited since they do not generate metastases in the brain [8–11]. The brain-metastasis field has attempted to overcome this challenge by injecting human $HER2^+$ breast-cancer cell lines or by implanting tumor tissues into immunodeficient mice that lack an intact adaptive immune system [12–14]. However, since interactions of cancer cells with components of the innate and adaptive immune system are critical for brain-metastasis development [15–17], these xenograft-based mouse models fail to adequately recapitulate the process of brain metastasis in humans. It is therefore imperative to generate tractable models of $HER2^+$ breast cancer that develop brain metastasis with high penetrance in immunocompetent mice in order to model the key aspects of brain metastasis that are observed in human patients. The development of such models can (i) provide valuable insights into important immune interactions in the brain microenvironment, (ii) accelerate the discovery of new immune-based therapies against brain metastasis, and (iii) be used to study HER2-therapy response and the subsequent development of resistance to HER2-targeting agents in breast-cancer brain metastases. In this study, we report the generation and validation of a new, experimental brain-metastatic model of $HER2^+$ breast cancer, which develops in a fully immunocompetent host.

Results

Generation of a $HER2^+$ brain-metastasis model in immunocompetent mice by in-vivo selection

To address the need for tractable immunocompetent models of brain metastasis in $HER2^+$ breast cancer, we used a murine estrogen receptor (ER)-negative, progesterone receptor (PR)-negative, murine HER2/neu-positive cell line (NT2.5) derived from a mammary tumor of the neu transgenic GEMM model originally isolated by the Sgouros laboratory [18]. We engineered the murine NT2.5 cell line to constitutively express both the luciferase gene for imaging and an antibiotic (blasticidin S) resistance gene. The luciferase-labeled NT2.5 cell line is denoted hereafter as the "neu-parental" line. To validate that these luciferase-labeled neu-parental cells maintained their ability to grow at the orthotopic site, we injected luciferase-labeled neu-parental cells into the mammary gland of syngeneic FVB/N mice. Once the tumors grew to a volume of 250 mm^3, we isolated, dissociated, and cultured the mammary tumors. We then purified cancer cells by antibiotic selection to eliminate the non-cancer cells of the tumor microenvironment. We subsequently injected the purified mammary cancer cells (denoted hereafter as "neu-primary" cells) into the arterial circulation of immunocompetent, syngeneic FVB/N mice via intracardiac injection (see schematic in Fig. 1A), which generated brain metastasis in 50% (3/6) of mice and extra-cranial metastases in 100% (6/6) of mice. Extra-cranial metastatic sites included liver, lung, and bone. To further enrich for highly brain-metastatic derivatives, we used the well-established serial passaging technique known as in-vivo selection [19]. To this end, we dissociated brain tissues from mice injected with neu-primary cells, purified the cancer cells by antibiotic selection, and re-injected them into new recipient FVB/N mice (Fig. 1A). By repeating this selection process five times, we obtained highly metastatic derivatives (denoted hereafter as "neu-BrM" cells) that efficiently metastasized to the brain in 12/12 (100%) mice upon intracardiac injection. In addition to brain metastasis, we observed extra-cranial metastasis to the liver in 10/12 mice, lung in 3/12 mice, and bone in 9/12 mice (Supplementary Fig. 1). For this study, we focused on brain metastasis, which was further confirmed both by ex-vivo bioluminescence imaging of the brain (Supplementary Fig. 1) and histological analysis of H&E-stained brain-tissue sections (Fig. 1B). Therefore, we have developed a tractable $HER2^+$ breast-cancer-metastasis mouse model by in-vivo selection, which efficiently grows in the brain in the presence of an intact immune system.

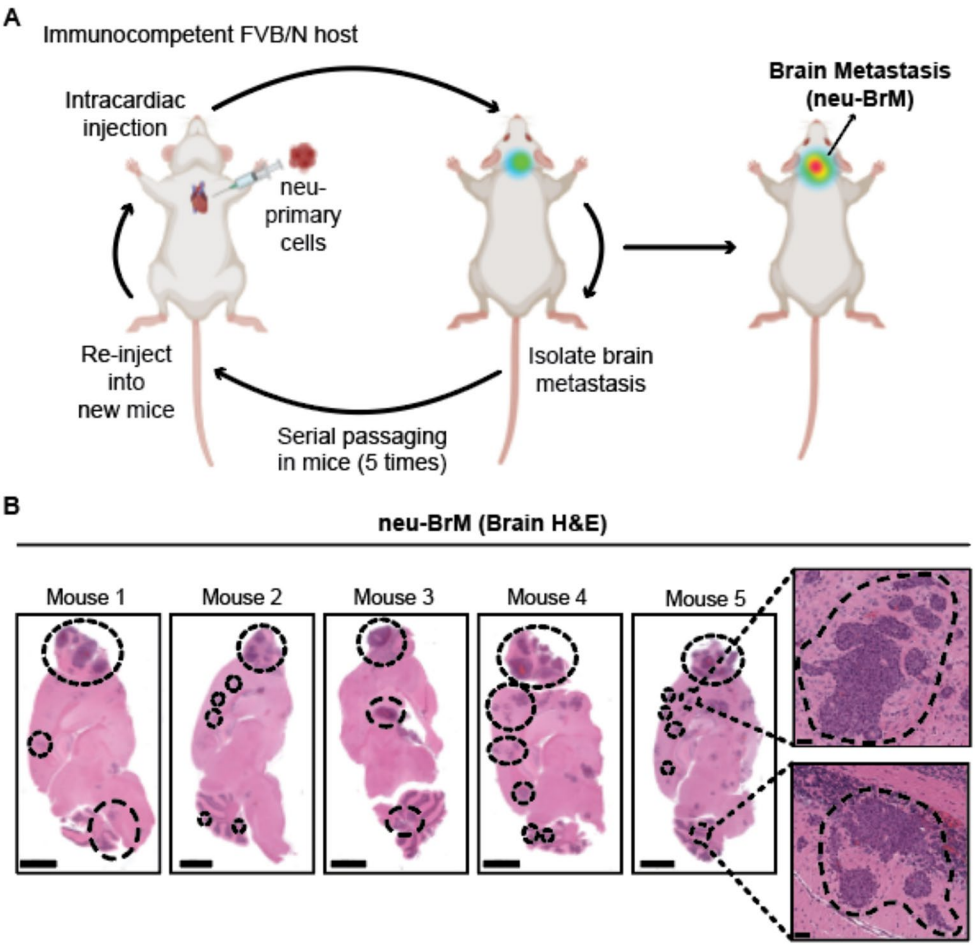

Fig. 1 Generation of a murine HER2$^+$ brain-metastasis model in immunocompetent mice by the process of in-vivo selection. (**A**) Schematic representation of the generation of brain-metastatic, murine neu-BrM cells by the process of in-vivo selection. Immunocompetent FVB/N mice were injected with luciferase-labeled, "neu-primary" tumor cells via intracardiac injection in the arterial circulation and monitored weekly by bioluminescence imaging. At endpoint, cancer cells were isolated from the brain and injected into new recipient mice for serial passaging. After five rounds of serial passaging, neu-BrM cells were obtained. Brain metastasis development was validated in three independent experiments. (**B**) Representative H&E images of brain-tissue sections from five mice harvested at 3 weeks following neu-BrM-tumor-cell injection into the arterial circulation. Dotted lines represent metastatic lesions in the brain in the indicated mouse. Scale bar for images on the left, 2000 µm. Zoomed insets on the right show magnified images of the metastatic lesions; scale bar for insets, 50 µm

Brain-metastatic cancer cells from the neu-BrM model maintain HER2 expression

Since HER2 expression levels in breast cancer cells are heterogeneous and varies during cancer progression [20], we next examined ERBB2 (murine HER2) expression in brain-metastatic lesions in the neu-BrM model. Immunohistochemical (IHC) analysis showed high HER2 expression in the brain-metastatic lesions from mice injected with neu-BrM cells (Fig. 2), although expression levels varied between cancer cells within the lesions. Similar to the neu-parental and neu-primary cell lines, neu-BrM cells lacked ER and PR expression and showed high *Erbb2* expression by qRT-PCR analysis (Supplementary Fig. 2). These results suggest that brain-metastatic lesions in the neu-BrM model maintain HER2 expression.

Prominent gliosis surrounding brain metastatic lesions in the neu-BrM model

A characteristic feature of human brain metastasis is reactive gliosis, in which astrocytes and microglial cells are activated in response to cancer cells in the brain [15, 21–24]. Analogous to human brain metastasis [21, 23], we observed prominent peritumoral gliosis around the brain metastatic lesions in the neu-BrM model (Fig. 3). Immunohistochemical analysis revealed a significant increase in the number of both GFAP-positive astrocytes and IBA1-positive microglia in the brain tissues of mice injected with neu-BrM cells compared to healthy control mice (Fig. 3A-B). Since the luciferase antigen can provoke an immune response in immunocompetent mice [25], we investigated whether the gliosis resulted from an increased immune reaction to the luciferase antigen expressed in cancer cells or from the growth of metastatic lesions in the brain. Our findings indicate that gliosis occurs in the brain tissues of mice injected with both luciferase-labeled and unlabeled neu-BrM (Fig. 3). This suggests that the gliosis is driven by the presence of tumor tissue rather than by an immune reaction to the luciferase antigen. Thus, similar to human patients with HER2+breast cancer, brain metastasis in the neu-BrM mouse model generates reactive gliosis due to outgrowth of cancer cells in the brain microenvironment.

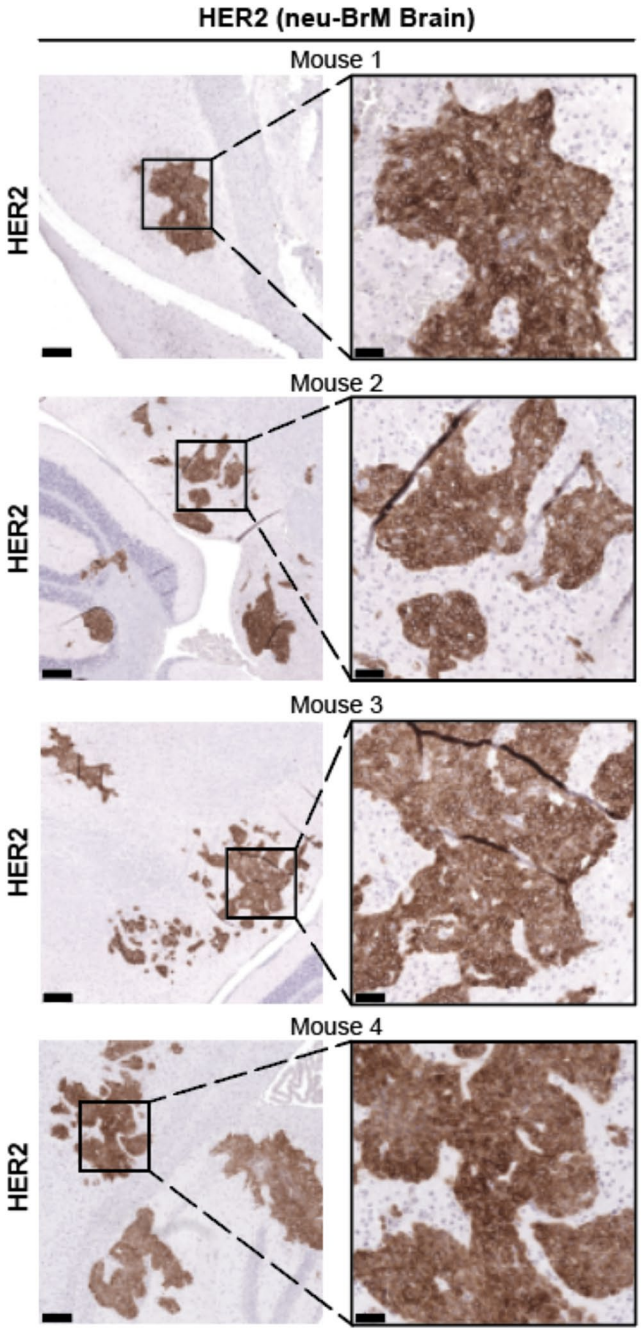

Fig. 2 Brain-metastatic cancer cells in the neu-BrM model maintain HER2 expression. Representative immunostained images using an antibody against HER2 on brain-tissue sections from four different mice at 3 weeks following neu-BrM-tumor-cell injection. Data representative of three independent experiments with n = 4-5 mice per group. Left images: scale bars, 200 µm. Images with zoomed inset on the right: scale bars, 50 µm

Increased infiltration of myeloid and CD4$^+$ T cells in neu-BrM-generated brain metastases

Since cancer-cell/immune interactions in the brain microenvironment play an important role in brain-metastasis development [15–17], we analyzed the immune-cell composition in brain-tissue sections from either mice bearing neu-BrM-derived brain metastasis or healthy controls by immunohistochemistry (Fig. 4). We observed a statistically significant increase in the number of F4/80$^+$ macrophages, S100A9$^+$ neutrophils, and CD4$^+$ T cells in the brain tissues of mice bearing brain metastases compared to those from control mice (Fig. 4A-B), which was reproducibly observed across different levels of brain tissue (Supplementary Fig. 3A-B). The infiltration of CD8$^+$ T cells and B220$^+$ B cells appeared to be modestly increased in the brain-metastatic lesions, although the data was not statistically significant (Supplementary Fig. 3C-D). Thus, analogous to human brain metastasis [26, 27], there is an increase in the number of infiltrating myeloid and CD4$^+$ T cells in the brains of mice bearing neu-BrM-induced brain metastases.

Pharmacological Inhibition of HER2 signaling by Tucatinib significantly reduces brain metastasis in the neu-BrM model

We next tested whether inhibiting HER2 signaling pharmacologically reduces brain-metastatic burden in the neu-BrM model. To this end, we utilized tucatinib, an FDA-approved HER2-targeting tyrosine kinase inhibitor. Tucatinib is used to treat unresectable or metastatic HER2-positive breast cancer and shows efficient blood-brain-barrier penetration [28–31]. We injected luciferase-labeled neu-BrM tumor cells into the arterial circulation of immunocompetent FVB/N mice via intra-cardiac injection. One week after the injection, mice were randomized and treated five days/week with either vehicle or tucatinib (100 mg/kg body weight/day by oral gavage) (see schematic in Fig. 5A). Compared to the vehicle-treated group, we observed a striking reduction in metastatic lesions in the brains of the tucatinib-treated group, although residual cancer cells persisted after the treatment period as potential seeds of relapse (Fig. 5B-C).

To determine the impact of tucatinib treatment on the immune cell composition in the neu-BrM model, we next analyzed brain-tissue sections from neu-BrM-injected mice treated with either vehicle or tucatinib and immunostained with F4/80, S100A9, or CD4 antibodies (Supplementary Fig. 4). We observed a statistically significant increase in the number of F4/80$^+$ macrophages in the tucatinib-treated group compared to the vehicle-treated group. However, we did not observe any significant changes in the number of S100A9$^+$ neutrophils or CD4$^+$ T cells in the brain tissues between the vehicle-treated and tucatinib-treated mice. Together, these results indicate that tucatinib treatment significantly reduces but does not eliminate brain metastasis in the neu-BrM model. Moreover, tucatinib treatment alters the number of specific immune subpopulation such

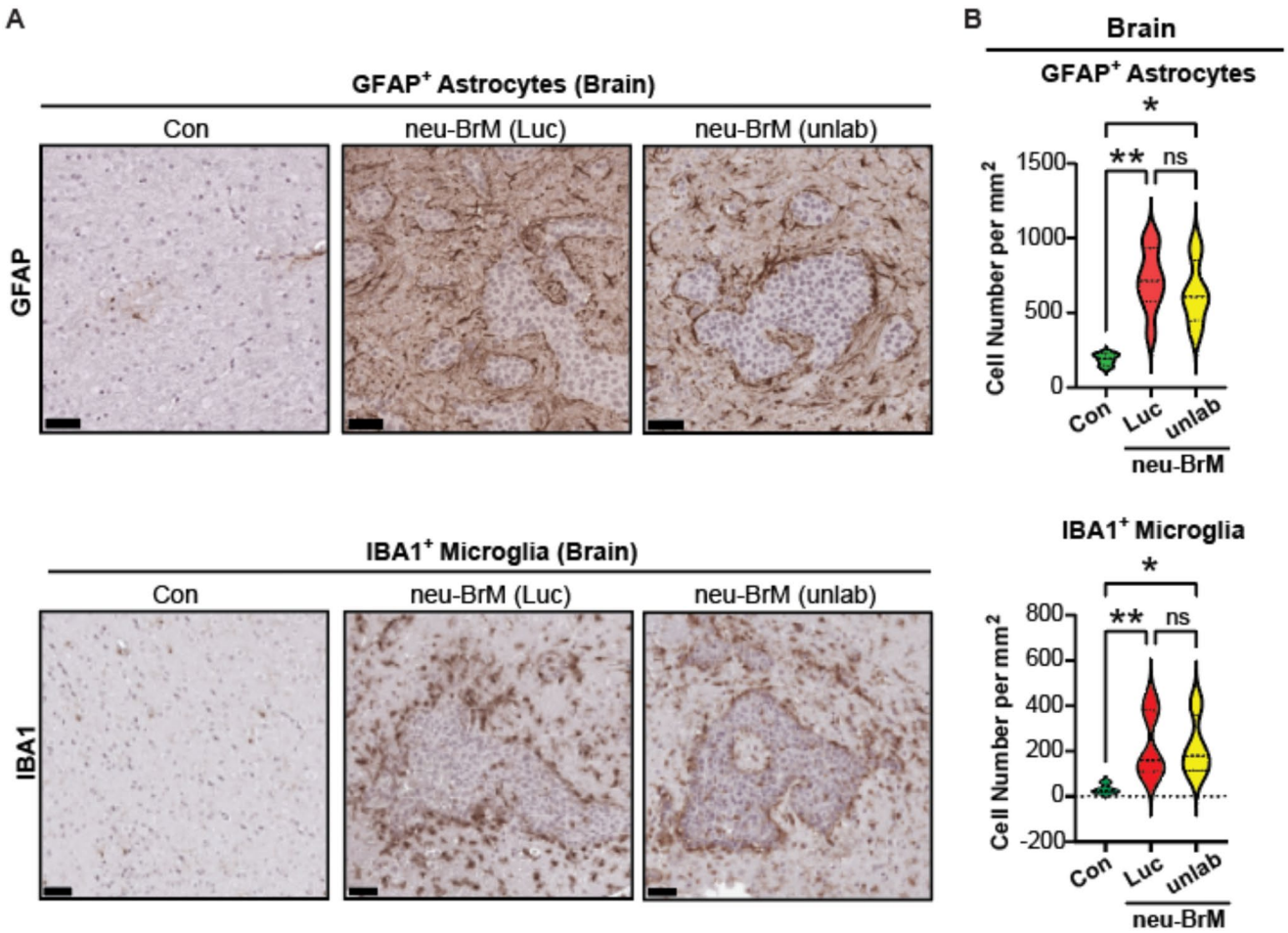

Fig. 3 Increased gliosis in neu-BrM-injected mouse brains compared to healthy mice. (**A**) Representative immunostained images using the indicated antibody on brain tissue sections from healthy, uninjected control ("Con"), or from mice at 3 weeks following tumor-cell injection with either neu-BrM expressing luciferase and an antibiotic marker ("neu-BrM Luc"), or neu-BrM expressing only an antibiotic marker and no luciferase ("neu-BrM unlab"). Scale bars = 50 µm. (**B**) Immunostained brain-tissue sections from (**A**) were quantified using automated QuPath software to identify cells that were positively stained with the indicated antibodies. $n=4$ for both Con and neu-BrM unlab groups. $n=8$ for neu-BrM Luc group. Data are presented as mean values ± SEM. *P*-values were determined by a two-tailed, unpaired, Mann–Whitney test. ** indicates $P=0.0087$, * indicates $P=0.0286$, and ns indicates not significant. Data is representative of three independent experiments with $n=4$-8 mice per group

as macrophages, which could be linked to their therapeutic responses. Therefore, these studies indicate that the neu-BrM model can serve as a useful resource for the metastasis community to study HER2-therapy response and resistance mechanisms and to identify drugs that can enhance the efficacy of HER2 therapy.

Discussion

The development of brain metastasis significantly shortens survival and reduces quality of life for HER2$^+$ breast cancer patients [32, 33]. Since available treatments fail to cure most patients with brain metastasis, disease progression continues to represent a major clinical challenge. Moreover, the discovery of new therapies for breast-cancer brain metastasis has been hindered by the lack of appropriate mouse models that reproducibly develop brain metastasis in the context of an intact immune system. The neu-BrM model that we present here addresses this experimental limitation and could serve as a valuable resource for the discovery of more effective and durable treatment regimens for HER2$^+$ breast cancer patients with brain metastasis.

Brain-metastasis development is a complex process that involves interactions between cancer cells and the cells of the brain microenvironment [1]. Consistent with human studies [21, 23], we observed reactive gliosis around neu-BrM-derived brain-metastatic lesions, with increased numbers of astrocytes and microglia. Since astrocytes and microglia have both pro- and anti-tumor functions [24, 34, 35], future studies can leverage the neu-BrM model

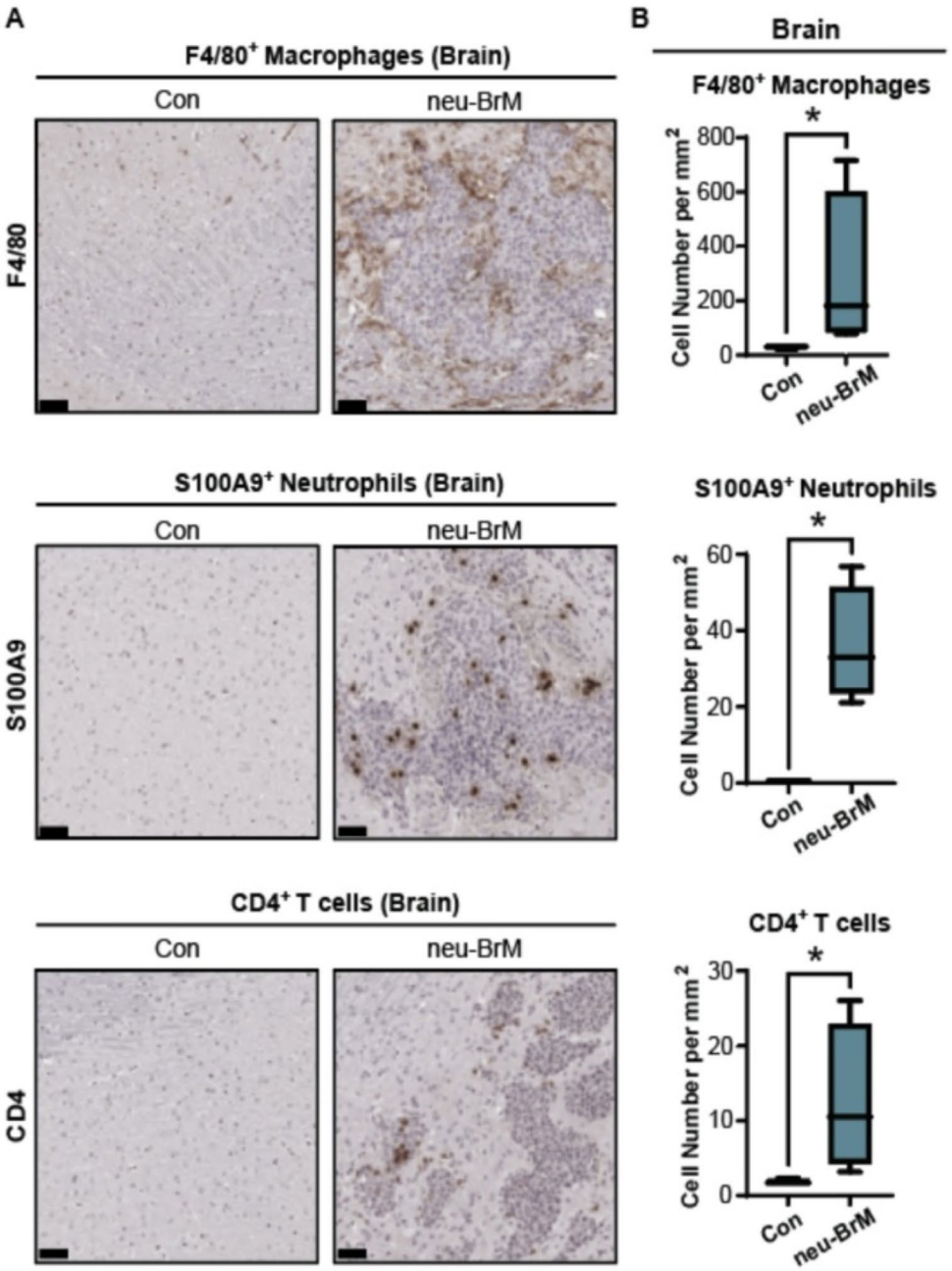

Fig. 4 Increased infiltration of myeloid and $CD4^+$ T cells in neu-BrM-generated brain metastases compared to brains from healthy mice. (**A**) Representative immunostained images using the indicated antibodies on healthy, uninjected control ("Con") brain-tissue sections or neu-BrM brain-tissue sections from mice at 3 weeks following neu-BrM-tumor-cell injection. Scale bars = 50 µm. (**B**) Immunostained brain-tissue sections from (**A**) were quantified using automated QuPath software to identify cells that were positively stained for the indicated antibodies. $n = 4$ for both Con and neu-BrM groups. Data are presented as mean values ± SEM. *P*-values were determined by a two-tailed, unpaired, Mann–Whitney test. * indicates $P = 0.0286$ for F4/80, S100A9, and CD4. Data is representative of two independent experiments with $n = 4$-5 mice per group

to interrogate the contribution of these cells during brain-metastasis progression.

One of the key advantages of using a fully immunocompetent mouse model for the study of brain metastasis is the presence of both innate and adaptive immune systems. Since B and T cells can impact brain-metastasis development [36], the neu-BrM model will be instrumental for exploring these processes. In the present study, we observed increased immune-cell infiltration in the brain of mice bearing neu-BrM metastases. In particular, the abundance of $F4/80^+$ macrophages, $S100A9^+$ neutrophils, and $CD4^+$ T cells increased compared to healthy brain, which is consistent with human studies [26, 27]. Interestingly, we also observed a trend toward increased infiltration of $CD8^+$ T cells in the brains of mice bearing neu-BrM metastases, which is generally associated with a good prognosis in human patients [27]. Therefore, it remains possible that the $CD8^+$ T cells are suppressed by myeloid cells in the milieu and are therefore unable to eliminate the cancer cells. Future studies will be needed to investigate the spatial localization, activation status, and function of the $CD8^+$ T cells in the context of the other immunosuppressive myeloid cells within the brain microenvironment.

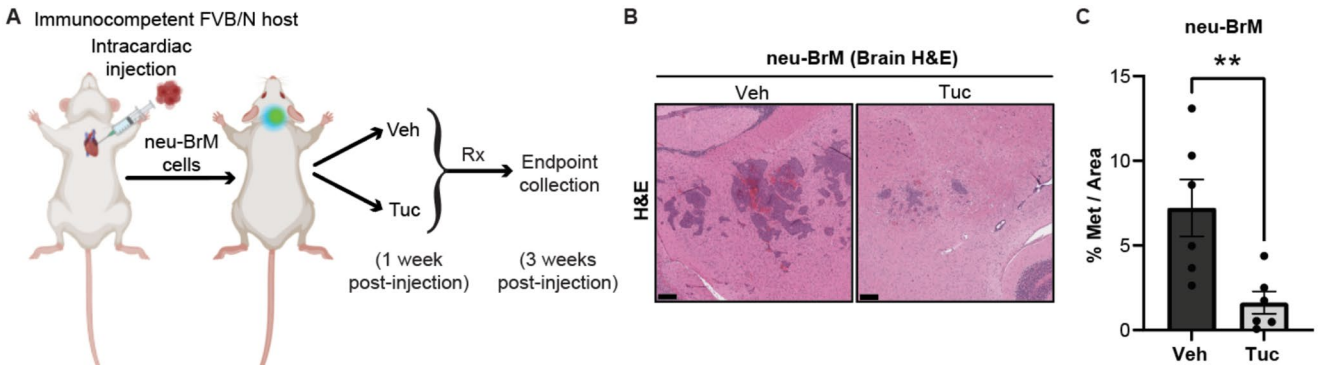

Fig. 5 Pharmacological inhibition of HER2 signaling by tucatinib significantly reduces brain metastasis in the neu-BrM model. (**A**) Schematic representation of the treatment regimen to examine the efficacy of tucatinib in reducing brain-metastatic lesions in the neu-BrM model. FVB/N mice were injected with luciferase-labeled neu-BrM tumor cells via intracardiac injection. Upon detection of brain-metastasis signal at 1 week post tumor-cell injection via bioluminescence imaging, mice were randomized to receive treatment by oral gavage with either vehicle ("Veh") or tucatinib ("Tuc") at 100 mg/kg body weight/day. At 3 weeks post tumor-cell injection, mice were euthanized, and brain tissues were harvested. (**B**) Representative H&E images of brain-tissue sections from the Veh-treated and Tuc-treated groups in (**A**). (**C**) Quantitative analysis of the percentage of metastasis area covered in the brain sections from (**B**). $n = 6$ for both Veh-treated brains and Tuc-treated brains. Data are presented as mean values ± SEM. P-values were determined by a two-tailed, unpaired Mann-Whitney test. ** indicates $P = 0.0087$. Data is representative of two independent experiments with $n = 4$-5 mice per group

The engineering of tumor cells to express luciferase has enabled the visualization of metastasis by longitudinal bioluminescence imaging in mice [37]. However, one of the limitations of using tumor-cell lines expressing luciferase in an immunocompetent murine host is the increased risk of immune-cell-mediated rejection of luciferase-expressing cancer cells [25]. Indeed, in the study by Song et al. [18], the luciferase-labeled NT2.5 cell line was rejected by immunocompetent neu-N transgenic mice, necessitating the use of immunocompromised nude mice to generate tumors from these cells. However, in our study, the luciferase-labeled neu-BrM brain metastasis cells were not rejected by the adaptive immune system, which enabled us to monitor both brain and extra-cranial metastasis over time. The difference in immune system response to the NT2.5 cell line between these two studies could be explained by differing mouse strains (neu-N transgenic mice in [18] versus FVB/N mice in our current study) and/or the threshold of luciferase expression [38] in these tumor cell lines.

A notable similarity between our immunocompetent neu-BrM model and the NT2.5-derived immunocompromised model generated by Song et al. [18] is that following a single intracardiac injection of NT2.5 cells without further selection, both models gave rise to a heavy burden of bone and liver metastasis and a relatively smaller burden of brain metastasis. However, through serial passaging of the NT2.5 cell line, we were able to select for increased severity and 100% penetrance of brain metastasis in the neu-BrM model. Therefore, the neu-BrM model could be utilized for understanding biological mechanisms of brain metastasis and for evaluating new targeting strategies against brain metastasis.

The experimental brain-metastasis models recapitulate the later steps of the brain-metastasis cascade that occur after cancer cells are in circulation. These crucial steps during brain-metastasis development include extravasation, survival, and outgrowth of cancer cells in the brain. Experimental brain-metastatic models of triple-negative breast cancer derived from 4T1-BR5 and firefly-luciferase- and GFP-labeled 4T1 cell lines have provided important insights into the colonization and growth of cancer cells in the brains of immunocompetent mice [39, 40]. Of relevance here, the Pouliot laboratory generated a single cell clone known as Primary Translational Breast Cancer Program-1 (TBCP-1) from a spontaneously arising murine mammary tumor cell line (called SMT-1) that was isolated by Judy Harmey's group [41]. The TBCP-1 clonal cell line was isolated using flow cytometry followed by long-term in-vitro culture. Importantly, TBCP-1 cells lack ER and PR expression and express high levels of ERBB2/HER2. Injection of the TBCP-1 cell lines led to the development of multi-organ metastasis in experimental metastasis assays in BALB/c mice [41]. Metastases arose in the bone and adrenal glands (90% incidence), kidneys and brain (80% incidence), and ovaries and liver (70% incidence). In contrast to the in-vitro single-cell clone isolation used to generate the TBCP-1 clone, the neu-BrM model described in our current study was created using the in-vivo selection (serial-passaging) strategy in mice, and intracardiac injection of the neu-BrM tumor cells generated brain metastases in 100% of FVB/N mice. Similar to the TBCP-1 model, the neu-BrM-injected mice also developed extra-cranial metastases (in the liver of 83% of mice, in the lungs of 25% of mice, and in the bones of 75% of mice). Therefore, the TBCP-1 metastasis model

developed by in-vitro clonal selection in BALB/c mice and our neu-BrM model developed by in-vivo selection in FVB/N mice are complementary and can be leveraged for mechanistic studies on metastasis and drug-efficacy studies in syngeneic mice.

Spontaneous metastasis models can be instrumental for studying the early stages of tumor-cell dissemination from the primary tumor. Although spontaneous metastasis from primary tumor models is often observed in visceral organs such as the lung and liver, metastasis to the brain using these models is rare. Consistently, Baugh et al. [42] developed a syngeneic metastatic model using the HER2/neu-expressing NT2.5 cell line (known as "NT2.5-LM") that metastasizes to the lung, liver, and bones (but not to the brain) after orthotopic mammary implantation in immunocompetent NeuN mice [42]. The Pouliot laboratory successfully created a brain-metastatic model by implanting TBCP-1 cells in the mammary gland and then resecting the tumor when it reached ~ 400 mm^3 [41], a strategy they successfully applied previously using the 4T1 Br4 murine TNBC model [43]. After surgical resection of the primary tumor, TBCP-1 tumor cells spontaneously metastasized to the lung and adrenal glands in 80% of mice, to the liver and ovary in 70% of mice, to the bone in 50% of the mice, and to the brain in 60% of mice where it grew as a single lesion. Future studies using the neu-BrM model will investigate whether, similar to the TBCP-1 study, (i) the neu-BrM model can spontaneously metastasize to the brain from the primary site, (ii) the incidence of brain metastasis increases after surgical resection of the primary tumors, and (iii) the metastasis pattern is altered by HER2-targeted therapies. The neu-BrM model is ultimately expected to serve as a useful resource for studying mechanisms of $HER2^+$ breast cancer brain metastasis that can be therapeutically exploited.

A recent advancement in HER2-targeted therapeutics is the development of blood-brain-barrier-(BBB)-penetrant treatments such as tucatinib [44]. Tucatinib has been FDA-approved for the management of $HER2^+$ metastatic breast cancer, including cases with brain metastasis [44, 45]. Although tucatinib has extended both progression-free and overall survival for patients with $HER2^+$ brain metastasis [45], drug resistance eventually arises followed by lethal relapses [46, 47]. Therefore, it is imperative to study and effectively target HER2-therapy-resistance mechanisms to prolong patient survival. Our studies demonstrate that, similar to human patients, brain-metastatic lesions in neu-BrM mice are sensitive to tucatinib inhibition; however, residual cancer cells still persist in the brain as potential seeds of relapse. The neu-BrM model can therefore serve as a useful tool for studying HER2-therapy response and resistance so that more effective therapeutics can emerge.

Methods

Cell culture

The neu-parental (NT2.5) cell line (unlabeled) was obtained from George Sgouros's lab [18] and was authenticated by PCR analysis for *Erbb2* overexpression and tested for mycoplasma contamination. STR profiling and interspecies contamination tests were performed at IDEXX. The neu-parental, neu-primary, and associated derivative brain-metastatic cell lines used in this study were cultured in DMEM media supplemented with 10% FBS and grown at 37 °C in a humidified 5% CO2 incubator. All media were supplemented with 100 IU/mL penicillin and 100 µg/mL streptomycin (Life Technologies).

Animal studies

All mouse protocols in this study were approved by the Columbia University Institutional Animal Care and Use Committee (IACUC) and were performed in compliance with the institutional guidelines of the Columbia University Irving Medical Center (CUIMC) Institute of Comparative Medicine. Treatments were conducted according to the ethical regulations and standards of the U.S. National Research Council's Guide for the Care and Use of Laboratory Animals and the U.S. Public Health Service's Policy on Humane Care and Use of Laboratory Animals. Mice were housed in the CUIMC Institute of Comparative Medicine barrier facility under conventional conditions with constant temperature and humidity and were provided with a standard diet (Labdiet 5053). In accordance with the IACUC guidelines from Columbia University, mice exhibiting a weight loss of 20% or more, a body-conditioning score (BCS) of 2 or less, or signs of hunched posture from cachexia, impaired locomotion, or respiratory distress were promptly euthanized. Euthanasia was performed by carbon-dioxide inhalation with a secondary method of cervical dislocation.

To generate brain-metastatic cell lines from neu-parental cells, female FVB/N mice aged 8 to 9 weeks (purchased from Jackson Laboratory) were used. The unlabeled NT2.5 (neu-parental) cells were engineered to express the blasticidin S antibiotic resistance gene, and the luciferase gene for bioluminescence imaging. As a non-luciferase control, we used neu-parental cells that were engineered to express the blasticidin S antibiotic resistance gene but not luciferase. The tumor cells were resuspended in Hank's Balanced Salt Solution (HBSS) for mammary-fat-pad injection. 5×10^5 NT2.5 (neu-parental) cells were injected in the fourth mammary gland in mice (orthotopic implantation) following our previous studies [48]. Tumor growth was monitored weekly using an electronic caliper to measure the length and width

of the tumors in millimeters. The tumor volume was calculated using the formula (length * (width^2)) / 2, where length and width represent the longest and shortest dimensions of the tumor, respectively. Mammary tumors were collected when they reached a size of 250 mm^3. Tumor tissues were dissociated with Dispase II (1 unit/mL, Roche) and Collagenase Type I (2 mg/mL, Worthington). Since the tumor cells expressed the blasticidin antibiotic resistance gene, 200 µg/mL of blasticidin S was added to the culture media to eliminate the non-tumor cells. These tumor cells were abbreviated as "neu-primary cells".

The tumor cells were resuspended in HBSS for intracardiac injection. The neu-primary cells were injected into new FVB/N mice (1×10^5 cells per mouse) via intracardiac injection into the arterial circulation. Metastasis was monitored weekly with an In Vivo Imaging System (AMI, Spectral Instruments Imaging). To measure bioluminescence, mice were anesthetized with 3-4% isoflurane and injected with 150 ng of D-Luciferin (Fisher Scientific) via intraperitoneal injections. Bioluminescence images were quantitated using Aura Software (Spectral Instruments Imaging), and total photon flux was calculated. Mice were weighed weekly and monitored twice a week.

Mice were euthanized, and metastatic organs with bioluminescence signal such as brain, liver, and lung were dissected. To isolate brain-metastatic cancer cells, the brain tissue was immediately cut into small pieces and incubated in 2.5 ml HBSS containing 2 unit/ml Dispase II and 2.5 mg/ml collagenase type 1 for 30 min at 37ºC with constant rocking. Subsequently, 10 ml of culture medium (DMEM + 10% FBS + penicillin-streptomycin) was added to enzyme-digested brain tissue, cells were collected as pellet by centrifugation (300xg for 5 minutes at room temperature), and the supernatant was discarded. After washing the cell pellet once with 10 ml of culture medium, the cells were transferred to a T25 cell-culture flask and kept in a CO_2-incubator at 37ºC. After 2 days, fresh culture medium containing selection antibiotic (200 µg/mL of blasticidin S) was added to select cancer cells that were stably transduced with lentivirus carrying the blasticidin-resistance gene. After 1–2 weeks of selection, the isolated tumor cells were re-injected into new FVB/N mice via intracardiac injection, a process that was repeated a total of 5 times to yield "neu-BrM". For rigor, we isolated brain-metastatic cancer cells from the brain tissues of 3–4 mice separately during each selection cycle. For each round, it took 1–2 weeks (depending on the size of the metastases) to culture the cells ex vivo with antibiotic selection to obtain sufficient brain-metastatic cancer cells for subsequent injection into mice. For all experiments involving the characterization and validation of neu-BrM, 1×10^5 cells were injected per mouse via intracardiac injection. For histological analysis of neu-BrM-tumor-bearing brain sections, mice were euthanized at 3 weeks post tumor-cell injection. Brain tissues were collected, fixed in 4% paraformaldehyde diluted in PBS for 24 h at 4 °C, and then washed with PBS before histological processing.

For drug experiments with neu-BrM, 1×10^5 neu-BrM cancer cells were injected per mouse via intracardiac injection in FVB/N mice as described above. For drug treatments, mice with neu-BrM were randomized to receive either vehicle or tucatinib treatment, following previous studies [47]. Tucatinib (Selleckchem) was diluted in 30% captisol and administered by oral gavage in mice with a dose of 100 mg/kg/day, 5 days a week. Treatment started at 1 week post tumor-cell injection and was continued for another 2 weeks (endpoint at 3 weeks post tumor-cell injection). All mice from both treatment groups survived until experimental endpoint. Mice were euthanized, and brain tissues were collected and fixed in 4% paraformaldehyde diluted in PBS for 24 h at 4 °C.

Immunostaining analysis

After washing in PBS, fixed mouse brain tissues were embedded in paraffin, and the blocks were sectioned at 5-µm thickness. Sections were analyzed from two different levels (50 microns apart) for each mouse. For immunostaining, slides were baked at 60 °C for 1 h and deparaffinized, rehydrated, and treated with 1% hydrogen peroxide for 10 min. Antigen retrieval was processed with pH-6.0 citrate buffer (Vector Laboratories) or pH-8.0 ethylenediaminetetraacetic acid (EDTA) in a steamer for 30 min. Slides were subsequently blocked with avidin- and biotin-blocking reagents (Vector Laboratories) for endogenous avidin and biotin for 15 min, respectively. BSA and goat serum were used as blocking agents for 30 min. The tumor slides were incubated with primary antibodies overnight at 4 °C, including rabbit antibodies against HER2 (1:500, Cell Signaling Technology), F4/80 (1:500, Cell Signaling Technology), S100A9 (1:500, Cell Signaling Technology), CD4 (1:200, Cell Signaling Technology), CD8 (1:200, Cell Signaling Technology), B220 (1:400, BD Pharmingen), GFAP (1:20,000, Agilent Dako), and IBA1 (1:20,000, Fujifilm), followed by incubation with anti-rabbit biotinylated secondary antibodies (1:250, Vector Laboratories). Detection of antibodies was performed using the ABC and DAB kits (Vector Laboratories). Slides were counterstained with hematoxylin, dehydrated, and mounted with Cytoseal XYL (Richard-Allan Scientific).

To calculate the number of positively stained cells per section, QuPath 0.5.0 software (https://qupath.github.io/) was applied to scanned images using methodology as previously described [49]. The image type was set as "Brightfield (H-DAB)", and the cell-detection channel was set at "Hematoxylin + DAB". Default values were used for nucleus and

intensity parameters. For cell detection with each antibody staining, the DAB threshold was optimized individually within the fast-cell-counts feature. For quantitation, the percentage of positively stained cells was determined by dividing the number of cells showing positive staining with a specific antibody by the surface area of the defined region of interest (ROI), measured in mm^2.

To calculate the percentage of area covered by metastasis in the brain sections, H&E-stained sections were analyzed using QuPath 0.5.0 methodology described previously [49]. The image type was set as "Brightfield H&E". Using the region-of-interest (ROI), and measure tools, we divided the area of the metastatic lesion by the total brain area under the field of view for each section to calculate the percentage of the area of brain sections covered by metastasis.

RNA isolation and qRT-PCR

Total RNA was isolated using TRIzol and an RNeasy Mini (Qiagen) Kit. 500 ng RNA was reverse-transcribed to cDNA using a cDNA Synthesis Kit (Roche). qRT-PCR was performed with 10 ng of cDNA per sample using gene-specific primers and SYBR Green PCR master mix (Applied Biosystems; Thermo Fisher Scientific). GAPDH primers were used as an internal control. qPCR was run using Applied Biosystems 7500 Real-Time PCR system (Applied Biosystems; Thermo Fisher Scientific), and the gene expression data were analyzed using the $2^{-\Delta\Delta Ct}$ method. The qRT-PCR primer sequences used in this study are shown below:

m*Erbb2*.

forward primer: 5-ACCGACATGAAGTTGCGACT C-3.

reverse primer: 5-AGGTAAGCTCCAAATTGCCC T-3.

m*Esr1*.

forward primer: 5-CCTCCCGCCTTCTACAGGT-3.

reverse primer: 5-CACACGGCACAGTAGCGAG-3.

m*Esr2*.

forward primer: 5-CTGTGATGAACTACAGTGTTC CC-3.

reverse primer: 5-CACATTTGGGCTTGCAGTCT G-3.

m*Pr*.

forward primer: 5-CTCCGGGACCGAACAGAGT-3.

reverse primer: 5-ACAACAACCCTTTGGTAGCA G-3.

m*Gapdh*.

forward primer: 5-AGGTCGGTGTGAACGGATTT G-3.

reverse primer: 5-TGTAGACCATGTAGTTGAGGT CA-3.

Statistical analysis

All statistical analyses were conducted using GraphPad Prism 10. Statistical methods for each experiment are described in the figure legends. All values were determined as the mean ± SEM. *P*-values < 0.05 were considered statistically significant.

Graphics

Graphics for the schematics were designed using Biorender.com with an institutional license to Columbia University Irving Medical Center (CUIMC).

Supplementary Information The online version contains supplementary material available at https://doi.org/10.1007/s10585-025-10343-4.

Acknowledgements We would like to thank Neil Vasan, Dawn Hershman, Henry Colecraft (CUIMC), and George Sgouros (Johns Hopkins University) for their feedback on our studies. We would like to extend our gratitude to patient advocates, Ms. Joan Mancuso and Ms. Deirdre Cossman, who have guided us in our studies. This work was supported by the METAvivor Foundation and Mary Kay Ash Foundation (to S. Acharyya). S. Acharyya was supported by the Pershing Square Sohn Award, HICCC and Irving Institute Pilot Awards funded through HICCC P30CA013696. M. Kandpal was supported in part by grant # UL1 TR001866 from the National Center for Advancing Translational Sciences (NCATS, National Institutes of Health (NIH) Clinical and Translational Science Award (CTSA) program. These studies utilized the resources from the Herbert Irving Comprehensive Cancer Center (HICCC) core facilities, which are funded in part through Center Grant P30CA013696.

Author contributions L. C. performed experiments leading to Figs. 1, 2, 3, 4 and 5 and co-wrote the manuscript. A. C.performed experiments leading to Figs. 1, 2, 3, 4 and 5 and co-wrote the manuscript.W.M performed experiments leading to figures 5 C. C. performed experiments leading to Figs. 1, 2, 3, 4 and 5. Y. G. performed experiments leading to Figs. 1 and 5. P. C. analyzed brain histopathology leading to Figs. 1, 2, 3, 4 and 5. M.K. performed power analysis and other statistical tests in figures 2-5. H. H. analyzed immunostaining analysis and provided histological evaluation leading to Figs. 1, 2, 3, 4 and 5. A. K. B. designed the experiments and and co-wrote the manuscript. S. A.

conceived the study, designed experiments, co-wrote the manuscript and supervised the study.

Data availability No datasets were generated or analysed during the current study.

Declarations

Competing interests The authors declare no competing interests.

References

1. Achrol AS et al (2019) Brain metastases. Nat Rev Dis Primers 5(1):5
2. Hosonaga M, Saya H, Arima Y (2020) Molecular and cellular mechanisms underlying brain metastasis of breast cancer. Cancer Metastasis Rev 39(3):711–720
3. Bendell JC et al (2003) Central nervous system metastases in women who receive trastuzumab-based therapy for metastatic breast carcinoma. Cancer 97(12):2972–2977
4. Pestalozzi BC et al (2008) Is risk of central nervous system (CNS) relapse related to adjuvant taxane treatment in node-positive breast cancer? Results of the CNS substudy in the intergroup phase III BIG 02–98 trial. Ann Oncol 19(11):1837–1841
5. Kennecke H et al (2010) Metastatic behavior of breast cancer subtypes. J Clin Oncol 28(20):3271–3277
6. Swain SM, Shastry M, Hamilton E (2023) Targeting HER2-positive breast cancer: advances and future directions. Nat Rev Drug Discov 22(2):101–126
7. Zimmer AS, Van Swearingen AED, Anders CK (2022) HER2-positive breast cancer brain metastasis: A new and exciting landscape. Cancer Rep (Hoboken) 5(4):e1274
8. Muller WJ et al (1988) Single-step induction of mammary adenocarcinoma in Transgenic mice bearing the activated c-neu oncogene. Cell 54(1):105–115
9. Guy CT et al (1992) Expression of the Neu protooncogene in the mammary epithelium of Transgenic mice induces metastatic disease. Proc Natl Acad Sci U S A 89(22):10578–10582
10. Moody SE et al (2002) Conditional activation of Neu in the mammary epithelium of Transgenic mice results in reversible pulmonary metastasis. Cancer Cell 2(6):451–461
11. Zheng L et al (2014) A model of spontaneous mouse mammary tumor for human Estrogen receptor- and progesterone receptor-negative breast cancer. Int J Oncol 45(6):2241–2249
12. Kabraji S et al (2023) Preclinical and clinical efficacy of trastuzumab Deruxtecan in breast cancer brain metastases. Clin Cancer Res 29(1):174–182
13. Gril B et al (2020) HER2 antibody-drug conjugate controls growth of breast cancer brain metastases in hematogenous xenograft models, with heterogeneous blood-tumor barrier penetration unlinked to a passive marker. Neuro Oncol 22(11):1625–1636
14. Valiente M et al (2020) Brain metastasis cell lines panel: A public resource of organotropic cell lines. Cancer Res 80(20):4314–4323
15. Quail DF, Joyce JA (2017) Microenvironmental Landsc Brain Tumors Cancer Cell 31(3):326–341
16. Gonzalez H et al (2022) Cellular architecture of human brain metastases. Cell 185(4):729–745e20
17. Adler O et al (2023) Reciprocal interactions between innate immune cells and astrocytes facilitate neuroinflammation and brain metastasis via lipocalin-2. Nat Cancer 4(3):401–
18. Song H et al (2008) An immunotolerant HER-2/neu Transgenic mouse model of metastatic breast cancer. Clin Cancer Res 14(19):6116–6124
19. Raz A, Hanna N, Fidler IJ (1981) Vivo isolation of a metastatic tumor cell variant involving selective and nonadaptive processes. J Natl Cancer Inst 66(1):183–189
20. Kotecha R et al (2021) Systematic review and meta-analysis of breast cancer brain metastasis and primary tumor receptor expression discordance. Neurooncol Adv 3(1):vdab010
21. Zhang M, Olsson Y (1995) Reactions of astrocytes and microglial cells around hematogenous metastases of the human brain. Expression of endothelin-like immunoreactivity in reactive astrocytes and activation of microglial cells. J Neurol Sci 134(1–2):26–32
22. Hasko J et al (2019) Response of the neurovascular unit to brain metastatic breast cancer cells. Acta Neuropathol Commun 7(1):133
23. Sambade MJ et al (2019) Examination and prognostic implications of the unique microenvironment of breast cancer brain metastases. Breast Cancer Res Treat 176(2):321–328
24. Ma W et al (2023) Type I interferon response in astrocytes promotes brain metastasis by enhancing monocytic myeloid cell recruitment. Nat Commun 14(1):2632
25. Jeon YH et al (2007) Immune response to firefly luciferase as a naked DNA. Cancer Biol Ther 6(5):781–786
26. Mitsuya K et al (2017) Elevated preoperative neutrophil-to-lymphocyte ratio as a predictor of worse survival after resection in patients with brain metastasis. J Neurosurg 127(2):433–437
27. Griguolo G et al (2022) A comprehensive profiling of the immune microenvironment of breast cancer brain metastases. Neuro Oncol 24(12):2146–2158
28. Criscitiello C et al (2023) Tucatinib's journey from clinical development to clinical practice: new horizons for HER2-positive metastatic disease and promising prospects for brain metastatic spread. Cancer Treat Rev 120:102618
29. Kaufman PA et al (2023) Real-world patient characteristics, treatment patterns, and clinical outcomes associated with Tucatinib therapy in HER2-positive metastatic breast cancer. Front Oncol 13:1264861
30. Frenel JS et al (2024) Tucatinib combination treatment after Trastuzumab-Deruxtecan in patients with ERBB2-Positive metastatic breast cancer. JAMA Netw Open 7(4):e244435
31. Guglielmi G et al (2024) Targeting HER2 in breast cancer with brain metastases: A Pharmacological point of view with special focus on the permeability of blood-brain barrier to targeted treatments. Eur J Pharmacol 985:177076
32. Niikura N et al (2014) Treatment outcomes and prognostic factors for patients with brain metastases from breast cancer of each subtype: a multicenter retrospective analysis. Breast Cancer Res Treat 147(1):103–112
33. Martin AM et al (2017) Brain metastases in newly diagnosed breast cancer: A Population-Based study. JAMA Oncol 3(8):1069–1077
34. Chen Q et al (2016) Carcinoma-astrocyte gap junctions promote brain metastasis by cGAMP transfer. Nature 533(7604):493–498
35. Evans KT et al (2023) Microglia promote anti-tumour immunity and suppress breast cancer brain metastasis. Nat Cell Biol 25(12):1848–1859
36. Mo H, Zhang X, Ren L (2024) Analysis of neuroglia and immune cells in the tumor microenvironment of breast cancer brain metastasis. Cancer Biol Ther 25(1):2398285
37. Dehaen N et al (2024) Luciferase transduction and selection protocol for reliable in vivo bioluminescent measurements in cancer research. Heliyon 10(13):e33356
38. Podetz-Pedersen KM et al (2014) Cellular immune response against firefly luciferase after sleeping beauty-mediated gene transfer in vivo. Hum Gene Ther 25(11):955–965

39. Lockman PR et al (2010) Heterogeneous blood-tumor barrier permeability determines drug efficacy in experimental brain metastases of breast cancer. Clin Cancer Res 16(23):5664–5678
40. Lorger M, Felding-Habermann B (2010) Capturing changes in the brain microenvironment during initial steps of breast cancer brain metastasis. Am J Pathol 176(6):2958–2971
41. Nagpal A et al (2019) Neoadjuvant neratinib promotes ferroptosis and inhibits brain metastasis in a novel syngeneic model of spontaneous HER2(+ve) breast cancer metastasis. Breast Cancer Res 21(1):94
42. Baugh AG et al (2024) A new Neu-a syngeneic model of spontaneously metastatic HER2-positive breast cancer. Clin Exp Metastasis 41(5):733–746
43. Kim SH et al (2018) *Identification of brain metastasis genes and therapeutic evaluation of histone deacetylase inhibitors in a clinically relevant model of breast cancer brain metastasis.* Dis Model Mech, 11(7)
44. Lin NU et al (2020) Intracranial efficacy and survival with Tucatinib plus trastuzumab and capecitabine for previously treated HER2-Positive breast cancer with brain metastases in the HER2CLIMB trial. J Clin Oncol 38(23):2610–2619
45. Murthy RK et al (2020) Tucatinib, trastuzumab, and capecitabine for HER2-Positive metastatic breast cancer. N Engl J Med 382(7):597–609
46. Sirhan Z, Thyagarajan A, Sahu RP (2022) The efficacy of tucatinib-based therapeutic approaches for HER2-positive breast cancer. Mil Med Res 9(1):39
47. Li R et al (2023) Tucatinib promotes immune activation and synergizes with programmed cell death-1 and programmed cell death-ligand 1 Inhibition in HER2-positive breast cancer. J Natl Cancer Inst 115(7):805–814
48. Tai Y et al (2024) FLT1 activation in cancer cells promotes PARP-inhibitor resistance in breast cancer. EMBO Mol Med 16(8):1957–1980
49. Biswas AK et al (2022) Targeting S100A9-ALDH1A1-Retinoic acid signaling to suppress brain relapse in EGFR-Mutant lung cancer. Cancer Discov 12(4):1002–1021